

Precise determination of fundamental parameters of six exoplanet host stars and their planets

K. Liu¹, S. L. Bi¹, T. D. Li^{1,2}, Z. E. Liu¹, Z. J. Tian¹ and Z. S. Ge¹

¹ Department of Astronomy, Beijing Normal University, Beijing 100875, China;
liukang@mail.bnu.edu.cn; bisl@bnu.edu.cn

² National Astronomical Observatories, Chinese Academy of Sciences, Beijing 100012, China;

Abstract The aim of this paper is to determinate the fundamental parameters of six exoplanet host (EH) stars and their planets. While techniques for detecting exoplanets yield properties of the planet only as a function of the properties of the host star, hence, we must accurately determine parameters of EH stars at first. For this reason, we constructed a grid of stellar models including diffusion and rotation-induced extra-mixing with given ranges of input parameters (i.e. mass, metallicity, and initial rotation rate). In addition to the commonly used observational constraints such as the effective temperature T_{eff} , luminosity L and metallicity [Fe/H], we added two observational constraints, the lithium abundance $\log N(\text{Li})$ and the rotational period P_{rot} . These two additional observed parameters can make further constrains on the model due to their correlations with mass, age and other stellar properties. Hence, our estimations of fundamental parameters for these EH stars and their planets are with higher precision than previous works. Therefore, the combination of rotational period and lithium help us to obtain more accurate parameters for stars, leading to an improvement of the knowledge of the physical state about the EH stars and their planets.

Key words: stars: fundamental parameters – stars: abundances – stars: evolution – stars: rotation – stars: planetary systems

1 INTRODUCTION

In the past two decades, thousands of identifiable planets outside the solar system have already been spotted (e.g. Vogt et al. , 2000; Pietrukowicz et al. , 2010; Moutou et al. , 2011; Ofir & Dreizler , 2013; Rowe et al. , 2014). An overwhelming majority of them have been discovered using indirect methods, i.e., radial-velocity (RV) and photometric transits. This is due to the fact that planets are non-luminous bodies, they merely reflects light of the parent star. A planet is like a small "undetectable" speckle in the stellar image, from a distance of a few parsec. But a planet can cause dynamical perturbations onto parent star, providing the possibility to detect it by indirect means. As a consequence, this makes the characteristic parameters of a exoplanet depend strongly and only on the characteristic parameters of the host star. Hence, it is of great significance to obtain the accurate masses and radii of host stars to study exoplanets (e.g. Seager & Mallén-Ornelas , 2003; Santos , 2008; Winn , 2010).

The most commonly used method for determination of the stellar properties is to fit the parameters of theoretical models with the observational constraints, e.g. effective temperature T_{eff} and luminosity L/L_{\odot} . However, this method generally makes it difficult to obtain sets of complete stellar atmospheric parameters. There are a few of free parameters in stellar structure and evolution models, which bring

more uncertainties in the observations, result in insufficient estimation of the stellar properties (Bi et al. , 2008).

Nevertheless, the abundance of lithium in stellar photospheres is usually used to study various processes, from big bang nucleosynthesis to the formation and evolution of planetary systems (e.g., Meléndez et al. , 2010; Santos et al. , 2010). Lithium is readily destroyed in stellar interiors at a comparatively low temperature ($\sim 2.5 \times 10^6$ K), therefore in solar-like stars, the surface lithium abundance was treated as an extremely sensitive diagnostic for stellar structure and evolution. Additionally, the evolution of lithium abundance during pre-MS and MS phases have strong correlations on several properties of star, i.e., metallicity, mass, age, and rotational history. Meanwhile, due to total angular momentum loss induced by magnetic braking, the rotational period of solar-like stars decreases with age during the main sequence. And the rate of angular momentum loss is related to stellar mass, radii and rotational rates. Accordingly, by combining non-standard stellar model which includes the process of extra-mixing with accurate measurement of lithium abundance and rotational period, we can obtain more precise estimation about the fundamental parameters of EH stars and their planets (do Nascimento et al. , 2009; Castro et al. , 2011; Li et al. , 2012).

In this work, we computed evolutionary models including rotation-induced element mixing and microscopic diffusion. We used three commonly used observation constraints (T_{eff} , L/L_{\odot} and $[\text{Fe}/\text{H}]$) and two additional observation constraints (the lithium abundance $\log N(\text{Li})$ and the rotational period P_{rot}) as restrictions of stellar models, aiming to provide the stellar parameters accurately. We assumed that the depletion of lithium happens at pre-main-sequence (pre-MS) and evolve differently with different initial rotational rates.

The observed data of the six EH stars and their planets are summarized in Section 2. The computational method and the details of our evolutionary models are described in Section 3. In Section 4, we present our modeling results and compare with previous studies. Finally, the discussion

2 THE SELECTION OF STAR SAMPLE

2.1 EH Stars

The sample stars for our modeling are six solar-analog stars with observed lithium abundances and rotational periods, and their planets have been detected by using radial-velocity. The detections of lithium abundances and rotational periods make it is possible to obtain precise estimations of stellar parameters, especially the masses and radii which are significant for us to determine the properties of their planets.

We summarized the observed data of EH stars which were used for our theoretical calculations in Table 1. The atmospheric features, T_{eff} , L , and $[\text{Fe}/\text{H}]$ were collected from Valenti & Fischer (2005), Ghezzi et al. (2010a), Israelian et al. (2004) and Baumann et al. (2010). We adopted the lithium abundance $\log N(\text{Li})$ from the observations of Ghezzi et al. (2010b), Israelian et al. (2004) and Baumann et al. (2010). The rotational period P_{rot} we used was determined by Wright et al. (2004) from the California and Carnegie Planet Search Program with the HIRES spectrometer at Keck Observatory. The average values of these observations were adopted in the following study.

The Spectra of Valenti & Fischer (2005) were obtained with the HIRES spectrograph mounted on the 10-m telescope at Keck Observatory (Vogt et al. , 1994), the UCLES spectrograph mounted on the 4-m Anglo-Australian Telescope at Siding Spring Observatory (Diego et al. , 1990), and the Hamilton echelle spectrometer at Lick Observatory (Vogt , 1987). The spectra of Ghezzi et al. (2010a,b) were obtained with the FEROS spectrograph mounted on the MPG/ESO 2.20-m telescope at La Silla (Kaufer et al. , 1999). The observations of Israelian et al. (2004) were carried out using the UES/4.2-m William Herschel, the SARG/3.5-m TNG at La Palma, and the FEROS/1.52-m ESO, the CORALIE/1.2-m Euler Swiss at La Silla. Stars from Baumann et al. (2010) were observed with RGT spectrograph mounted on the 2.7-m Harlan Smith telescope at the McDonald observatory, MIKE spectrograph mounted on the 6.5-m Magellan Clay telescope at Las Campanas observatory, and HARPS spectrograph mounted on the 3.6-m ESO telescope at La Silla observatory.

Table 1 Main Characteristics of Six EH Stars.

HIP	HD	T_{eff} (K)	$\log(L/L_{\odot})$	[Fe/H]	$\log N$ (Li) (dex)	P_{rot}	ref
9683	12661	5743±44	0.093±0.063	0.36±0.03	(1)
		5785±50	0.033±0.063	0.37±0.03	1.10±0.60	...	(2)
		5715±70	...	0.36	(3)
		35±2.1	(5)
		5748±70	0.063±0.063	0.36±0.03	1.10±0.60	35±2.1	(6)
	
33212	50554	5929±44	0.167±0.063	-0.07±0.03	(1)
		5982±26	0.119±0.062	-0.07±0.02	2.40±0.11	...	(2)
		6050±70	...	0.02	2.59	...	(3)
		16±1.0	(5)
		5987±70	0.143±0.063	-0.04±0.03	2.50±0.11	16±1.0	(6)
47007	82943	5997±44	0.169±0.047	0.27±0.03	(1)
		6011±36	0.152±0.061	0.28±0.03	2.47±0.10	...	(2)
		6025±70	...	0.33	2.52	...	(3)
		20±1.2	(5)
		6011±70	0.161±0.061	0.29±0.03	2.50±0.10	20±1.2	(6)
50473	89307	5898±44	0.096±0.062	-0.16±0.03	(1)
		5914±25	0.130±0.063	-0.18±0.02	2.18±0.11	...	(2)
		18±1.1	(5)
		5906±44	0.113±0.063	-0.17±0.03	2.18±0.11	18±1.1	(6)
59610	106252	5870±44	0.107±0.069	-0.08±0.03	(1)
		5923±38	0.108±0.063	-0.05±0.03	1.69±0.13	...	(2)
		5890±70	...	-0.01	1.65	...	(3)
		5899±62	...	-0.034±0.041	1.71±0.04	...	(4)
		23±1.4	(5)
		5896±70	0.108±0.069	-0.04±0.04	1.68±0.13	23±1.4	(6)
77740	141937	5847±44	0.070±0.073	0.13±0.03	(1)
		5842±36	-0.026±0.067	0.10±0.03	2.26±0.11	...	(2)
		5925±70	...	0.11	2.48	...	(3)
		5900±19	...	0.125±0.030	2.36±0.02	...	(4)
		21±1.3	(5)
		5879±70	0.022±0.073	0.12±0.03	2.37±0.11	21±1.3	(6)

Reference: (1) Valenti & Fischer (2005); (2) Ghezzi et al. (2010a) and Ghezzi et al. (2010b); (3) Israelian et al. (2004); (4) Baumann et al. (2010); (5) Wright et al. (2004); (6) Mean value.

2.2 Exoplanets

We listed the planetary orbital parameters which were obtained by RV measurements in Table 2. Two of these systems are found multi-planetary. HD 12661 and HD 82943 host two and three planets, respectively. Orbital period P , eccentricity e , and semi-amplitude K_1 (the velocity wobble) were gave here, for more details about the planetary such as the periastron passage time T and the angle between the periastron and the line-of-nodes ω can be found in the related literatures.

The radial velocity data were from the HIRES spectrograph (HD 12661 and HD 82943) mounted on 10-m Keck-1 telescope at the Keck Observatory (Vogt et al. , 1994), the ELODIE echelle spectrograph (HD 50554 and HD 106252) and the SOPHIE spectrograph (HD 89307) mounted on the Cassegrain focus of the 1.93-m telescope at Haute-Provence Observatory (Baranne et al. , 1996), and the CORALIE echelle spectrograph (HD 141937) mounted on the 1.2-m Euler Swiss telescope at La Silla Observatory (Queloz et al. , 2000; Udry et al. , 2000), respectively.

Table 2 Main Characteristics of Exoplanets.

Planet	P (day)	e	K_1 (m s^{-1})	Ref
HD 12661b	262.709 ± 0.083	0.3768 ± 0.0077	73.56 ± 0.56	(1)
HD 12661c	1708.0 ± 14.0	0.031 ± 0.022	30.41 ± 0.62	(1)
HD 50554b	1293.0 ± 37.0	0.501 ± 0.030	104 ± 5	(2)
HD 82943b	442.4 ± 3.1	0.203 ± 0.052	39.8 ± 1.3	(3)
HD 82943c	219.3 ± 0.8	0.425 ± 0.018	54.4 ± 2.0	(3)
HD 82943d	1072 ± 13	0 ± 0	5.39 ± 0.57	(4)
HD 89307b	2199 ± 61	0.25 ± 0.09	32.4 ± 4.5	(5)
HD 106252b	1600.0 ± 18.0	0.471 ± 0.028	147 ± 4	(2)
HD 141937b	653.22 ± 1.21	0.41 ± 0.01	234.5 ± 6.4	(6)

Reference: (1) Wright et al. (2009); (2) Perrier et al. (2003); (3) Tan et al. (2013); (4) Baluev & Beaugé (2014); (5) Boisse et al. (2012); (6) Udry et al. (2002).

3 STELLAR MODELS

3.1 Input Physics

To estimate the parameters of the sample stars, a grid calculation were carried out based on a stellar evolutionary model named Yale Rotating Stellar Evolution Code (YREC) (Pinsonneault et al. , 1990, 1992; Demarque et al. , 2008), which includes diffusion, angular momentum loss, angular momentum transport and rotation-induced elements mixing. Detailed descriptions of model can be found in Guenther et al. (1992), Chaboyer et al. (1995) and Li et al. (2003). The calculations were carried out with the up-to-date OPAL equation-of-state tables EOS2005 (Rogers et al. , 2002). Solar mixture of GS98 (Grevesse et al. , 1998) ($Z_{\odot} = 0.0170$ and $(Z/X)_{\odot} = 0.0230$) was adopted and hence the opacities were generated with the composition of GS98 (Grevesse et al. , 1998) and supplemented by low-temperature opacities from Ferguson et al. (2005). Atmosphere of the model follows the Eddington $T - \tau$ relation. We used NACRE reaction rates (Angulo et al. , 1999) for nuclear reaction and the mixing length theory (Böhm-Vitense , 1958) for convection. Following the formulation of Thoul et al. (1994), the gravitational settling of helium and heavy elements is considered in the stellar model.

When rotation is taken into account, the characteristics of a model depend on six parameters: mass M , age t , mixing-length parameter $\alpha \equiv l/Hp$, two parameters: X_{ini} and Z_{ini} described the initial chemical composition of a star, and rotational period P_{rot} . To reproduce the evolution of lithium, evolutions of stars during Pre-MS stage is considered and hence we selected the initial model for each calculation on the Hayashi Line. All of the models evolved to exhaust its supply of the hydrogen in the core. Initial helium abundance ($Y_{\text{ini}} = 0.275$) and the mixing-length parameter ($\alpha = 1.75$) were regarded as constants in the grid computation.

The ranges of variable parameters of the grid calculation and their step sizes are shown in Table 3. According to the effective temperatures of the sample stars, we set the range of mass from 0.90 to $1.10 M_{\odot}$ with a grid size of $0.01 M_{\odot}$. The range of mass fraction of all heavy elements Z_{ini} , which was derived from Z_{\odot} and the observed $[\text{Fe}/\text{H}]$, is from 0.010-0.040 dex with a grid size of 0.001 dex. Although the initial models were selected on the Hayashi Line, we used the rotational rates at zero age main sequence (V_{ZAMS}) to represent the rotational conditions for better understanding. The range of V_{ZAMS} is from 20 to 70 km s^{-1} , in steps of 10 km s^{-1} .

Table 3 Input Parameters for Theoretical Calculation.

Variate	MIN	MAX	δ^a
$M(M_\odot)$	0.90	1.10	0.01
Z	0.010	0.040	0.001
V_{ZAMS} (km s ⁻¹)	20	70	10

Notes: ^a The value of δ represents the increment between the minimum and maximum values.

3.2 Angular Momentum Loss

The braking law of Kawaler (1988) is adopted as the angular momentum loss equation:

$$\frac{dJ}{dt} = \begin{cases} -K\Omega^3(R/R_\odot)^{1/2}(M/M_\odot)^{-1/2}(\Omega \leq \Omega_{\text{sat}}) \\ -K\Omega\Omega_{\text{sat}}^2(R/R_\odot)^{1/2}(M/M_\odot)^{-1/2}(\Omega > \Omega_{\text{sat}}), \end{cases} \quad (1)$$

where the parameter K is constant for all stars, and associated with the magnetic field intensity. Ω_{sat} is the angular velocity of surface when the magnetic saturation occurs in star. Both K and Ω_{sat} are free parameters and we follow Bouvier et al. (1997) setting $K = 2.0 \times 10^{47}$ g cm² s and $\Omega_{\text{sat}} = 14 \Omega_\odot$.

3.3 Extra-mixing in the Radiative Region

Besides the microscopic diffusion of elements, which we have mentioned above, angular momentum transport and elements mixing caused by rotation are taken into account in radiative regions. These processes can be described as a couple of diffusion equations (Chaboyer et al. , 1995):

$$\rho r^2 \frac{I}{M} \frac{d\Omega}{dt} = \frac{d}{dr} \left(\rho r^2 \frac{I}{M} D_{\text{rot}} \frac{d\Omega}{dt} \right), \quad (2)$$

$$\rho r^2 \frac{dX_i}{dt} = \frac{d}{dr} \left[\rho r^2 D_{m,1} X_i + \rho r^2 (D_{m,2} + f_c D_{\text{rot}}) \frac{dX_i}{dt} \right], \quad (3)$$

where Ω is the angular velocity, X_i is the mass fraction of chemical species i , and I/M is the moment of inertia per unit mass. $D_{m,1}$ and $D_{m,2}$ are the microscopic diffusion coefficients. D_{rot} is the diffusion coefficient caused by rotation-induced mixing. More details of these diffusion coefficients were given by Chaboyer et al. (1995). The tunable parameter f_c was used to alter the effects of rotation-induced element mixing. It was determined by observations, that is, the depletion of lithium in our solar model must fits the observed depletion in Sun (Chaboyer et al. , 1995).

4 RESULTS

4.1 Stellar Parameters

we calculated a series of evolutionary models in estimated M and Z_{ini} ranges to reproduce the observational constraints of these six EH stars. As shown in Fig. 1, evolutionary tracks for each stars are plotted in conformity to observational constraints. For the sake of simplicity, the situations of star HD 12661 is taken as an example.

First of all, three classical observed features, the effective temperature T_{eff} , luminosity L and metallicity $[\text{Fe}/\text{H}]$, were considered and 157 tracks are found fitting these three observational constraints. The mass and age of HD 12661 provided by the models are $1.02 \pm 0.03 M_\odot$ and 6.76 ± 4.31 Gyr.

Secondly, lithium abundance was taken into account. Lithium is the most important element since it is readily burned in the stellar interiors. The abundance of lithium indicates the extent of element mixing in the stars, in addition, the depletion of lithium depends strongly on the mass and age of star (do Nascimento et al. , 2009; Li et al. , 2012). In this step, there are only 76 evolutionary tracks which

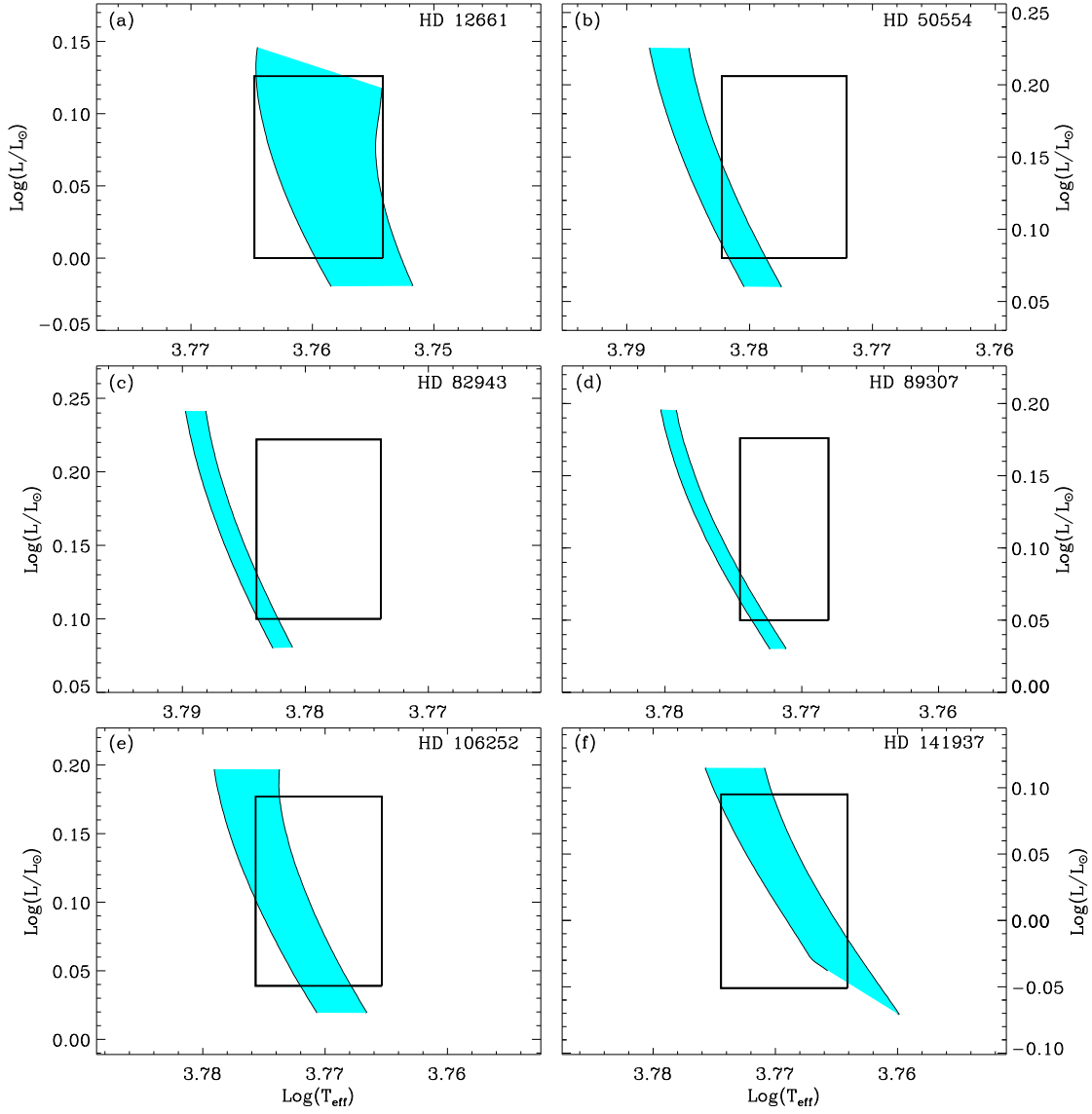


Fig. 1 Evolutionary tracks of HD 12661, HD 50554, HD 82943, HD 89307, HD 106252, and HD 141937 in the H-R diagram constrained by a) $T_{\text{eff}} + L + [\text{Fe}/\text{H}]$; b) $T_{\text{eff}} + L + [\text{Fe}/\text{H}] + \log N(\text{Li})$; c) $T_{\text{eff}} + L + [\text{Fe}/\text{H}] + \log N(\text{Li}) + P_{\text{rot}}$.

fit four observational constraints, including lithium abundance $\log N(\text{Li})$, and we estimate the mass and age of the star HD 12661 are $1.02 \pm 0.02 M_{\odot}$ and 5.56 ± 3.01 Gyr. Additionally, lithium abundance narrows the ranges of input parameters, thus the possible position of the star in the H-R diagram is restricted to a smaller field than what has been obtained above.

Finally, after adding the rotational period to our models as a constraint, only 30 evolutionary tracks are found fitting the observed P_{rot} . The range of V_{ZAMS} is significantly reduced to $30 \text{ km s}^{-1} - 40 \text{ km s}^{-1}$. In a same way as lithium abundance, the ranges of input parameters of the stellar models are also reduced by the rotational period, and hence it makes further constraining to the possible position of the star in the H-R diagram as shown in Fig. 1a. The rotational period P_{rot} helps us determinate the mass and age of HD 12661 even more precisely, which are $1.02 \pm 0.02 M_{\odot}$ and $6.39 \pm 1.94 \text{ Gyr}$.

The same method were adopted for all the other EH stars, we plotted their evolutionary tracks in Fig. 1, each line illustrate the each star. Comparing the situation of star HD 12661 with others, we find that this star occupy larger area in H-R diagram than five other stars in Fig. 1, this is owing to a large error in the abundance of lithium for HD 12661.

4.2 Comparison with Previous Results

These six EH stars were previously studied by several researchers, the methods and estimates of two of them could be seen in Table 4. Ghezzi et al. (2010a) and Valenti & Fischer (2005) observed these stars and provided their masses, radii and ages through different methods. We compare their results obtained by interpolating isochrones with ours in the following paragraphs. The comparisons of masses and ages of these six EH stars were plotted in Fig. 2.

For the six EH stars, the results of Ghezzi et al. (2010a) given the error of mass is $\sim 0.10 M_{\odot}$ and the error of age is $\sim 2.0 \text{ Gyr}$. The mass determinations of Valenti & Fischer (2005) were close to those of Ghezzi et al. (2010a) but with higher precision, i.e., $\Delta M \sim 0.05 M_{\odot}$. Our mass estimations of HD 12661, HD 50554, HD 82943, HD 89307, HD 106252, and HD 141937 are $1.02 \pm 0.02 M_{\odot}$, $1.04 \pm 0.01 M_{\odot}$, $1.04 \pm 0.01 M_{\odot}$, $1.05 \pm 0.01 M_{\odot}$, $1.03 \pm 0.03 M_{\odot}$, and $1.03 \pm 0.02 M_{\odot}$, respectively, most of which are less massive than what have been obtained by Ghezzi et al. (2010a) and Valenti & Fischer (2005). This result is due to the element transport which caused by the interaction between diffusion and rotation-induced mixing in the stellar radiative region (Chaboyer et al. , 1995; Eggenberger et al. , 2010). The process of element transport changes the chemical composition of the external layers and hence cause the evolutionary tracks shift to hot side on the H-R diagram. Thus, when the observed effective temperature is given, rotational model tends to provide less massive result of mass than those obtained by standard model. The precision of our mass determinations is the best of the three, which is $0.01 \sim 0.03$.

Ages of these six EH stars provided by Valenti & Fischer (2005) are mostly older than those of Ghezzi et al. (2010a), with a similar accuracy, i.e., $\Delta t \sim 2.0 \text{ Gyr}$. Our age determinations generally agree within the errors of previous works, and which are much more accurate ($\Delta t \sim 0.5 \text{ Gyr}$) than determined by interpolating isochrones. (see Table 4). Moreover, Combining the rotational periods listed in Table 1 with ages obtained by us, we found that there is a positive correlation between them.

This result is reasonable, because the depletion of lithium is a function of stellar mass, age, rotational rates and metallicity, while the rotational period increases with age during the main sequence. Therefore, these two additional observational constraints can effectively restrict the ranges of input parameter and improve the precision of the stellar model.

4.3 Planetary Parameters

For a given planetary system with known orbital parameters, we can calculate the mass function(Santos , 2008):

$$f(m) = \frac{(M_2 \sin i)^3}{(M_1 + M_2)^2} = 1.036 \times 10^{-7} K_1^3 (1 - e^2)^{(3/2)} P \quad (4)$$

where M_1 and M_2 are the masses of the star and planet, i is the inclination of the line of sight with respect to the orbital axis, K_1 is the semi-amplitude of radial-velocity of the star with mass M_1 , e is the orbital eccentricity, and P is orbital period.

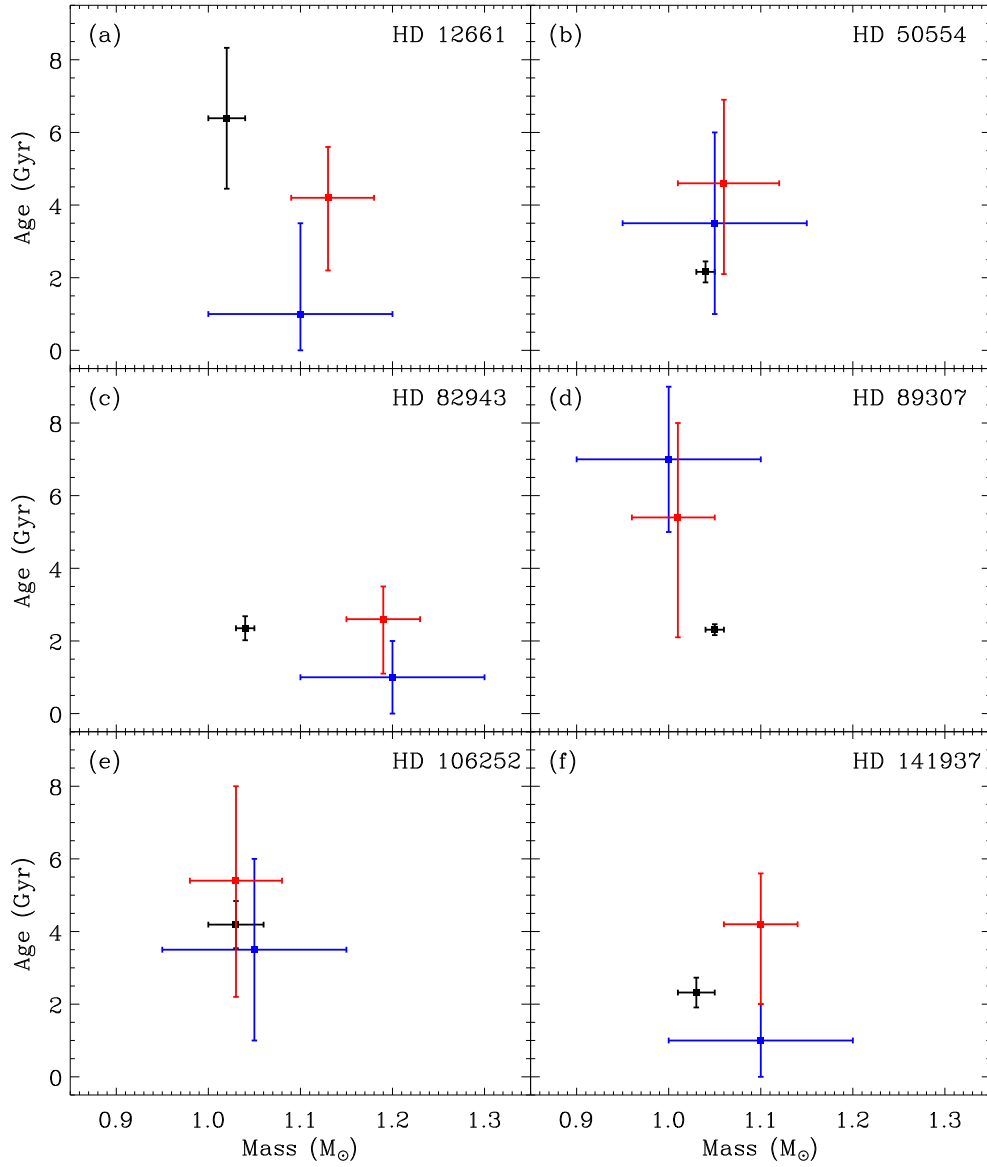


Fig. 2 Comparisons between masses and ages determined by our model (the black error bar) and estimates of previous studies for all six EH stars. The red and blue error bars represent the results of Valenti & Fischer (2005) and Ghezzi et al. (2010a), respectively.

Furthermore, as we know, from Kepler's third law:

$$\frac{a^3}{P^2} = \frac{G(M_1 + M_2)}{4\pi^2} \quad (5)$$

where a is orbital semimajor axis and G is the universal gravitational constant.

Table 4 Stellar Parameters and Comparison with Previous Studies.

Star	M (M_{\odot})	t (Gyr)	R (R_{\odot})	Method	Ref.
HD 12661	0.96±0.47	...	1.04±0.08	Spectroscopic	(1)
	1.10±0.10	1.0 ^{+2.5} _{-1.0}	...	Isochrones	(1)
	1.22±0.18	...	1.124±0.037	Spectroscopic	(2)
	1.13 ^{+0.05} _{-0.04}	4.2 ^{+1.4} _{-2.0}	...	Isochrones	(2)
	1.02±0.02	6.39±1.94	1.11±0.08	This work	
HD 50554	0.81±0.39	...	1.07±0.08	Spectroscopic	(1)
	1.05±0.10	3.5 ^{+2.5} _{-2.5}	...	Isochrones	(1)
	0.93±0.14	...	1.149±0.039	Spectroscopic	(2)
	1.06 ^{+0.06} _{-0.05}	4.6 ^{+2.3} _{-2.5}	...	Isochrones	(2)
	1.04±0.01	2.16±0.29	1.02±0.02	This work	
HD 82943	1.03±0.50	...	1.10±0.09	Spectroscopic	(1)
	1.20±0.10	1.0 ^{+1.0} _{-1.0}	...	Isochrones	(1)
	1.22±0.17	...	1.125±0.029	Spectroscopic	(2)
	1.19 ^{+0.04} _{-0.04}	2.6 ^{+0.9} _{-1.5}	...	Isochrones	(2)
	1.04±0.01	2.35±0.33	1.03±0.02	This work	
HD 89307	0.85±0.41	...	1.11±0.09	Spectroscopic	(1)
	1.00±0.10	7.0 ^{+2.0} _{-2.0}	...	Isochrones	(1)
	0.91±0.13	...	1.069±0.035	Spectroscopic	(2)
	1.01 ^{+0.04} _{-0.05}	5.4 ^{+2.6} _{-3.3}	...	Isochrones	(2)
	1.05±0.01	2.31±0.15	1.01±0.01	This work	
HD 106252	1.16±0.57	...	1.08±0.09	Spectroscopic	(1)
	1.05±0.10	3.5 ^{+2.5} _{-2.5}	...	Isochrones	(1)
	1.01±0.15	...	1.093±0.040	Spectroscopic	(2)
	1.03 ^{+0.05} _{-0.05}	5.4 ^{+2.6} _{-3.2}	...	Isochrones	(2)
	1.03±0.03	4.19±0.65	1.05±0.01	This work	
HD 141937	0.58±0.28	...	0.95±0.08	Spectroscopic	(1)
	1.10±0.10	1.0 ^{+1.0} _{-1.0}	...	Isochrones	(1)
	1.07±0.13	...	1.056±0.039	Spectroscopic	(2)
	1.10 ^{+0.04} _{-0.04}	4.2 ^{+1.4} _{-2.2}	...	Isochrones	(2)
	1.03±0.02	2.32±0.41	0.99±0.06	This work	

Reference: (1) Ghezzi et al. (2010a); (2) Valenti & Fischer (2005).

From Equation 4 and 5, and combined stellar masses determined in the previous section, the minimum masses $M_2 \sin i$ and orbital semimajor axes a of planets can be obtained, as shown in Table 5. It should be noted that the uncertainty of our estimation consists of two parts. One is associated with the observation, such as the errors of P , e , and K_1 (listed in Table 2). The other is produced by the model, specifically, the error of stellar mass. We summarized the two parts of the uncertainty separately in Table 5. Compared with the results of previous studies, our determinations are more accurate, whether including the errors of observations or not.

Batalha et al. (2013) pointed out that a $0.1 M_{\odot}$ companion would induce a systematic error of approximately 2%. Correspondingly, the accuracy and precision of parameters of EH star will have a huge impact on our estimates of properties of planet. Therefore, the accurate knowledge of EH star is extremely important for the study of exoplanets.

Table 5 Planetary Parameters and Comparison with Previous Studies.

Planet	Previous Studies			This Work					
	$M \sin i$ (M_{Jup})	a (AU)	Ref	$M \sin i$ (M_{Jup})	δ_M^{obs} (M_{Jup})	δ_M^{theo} (M_{Jup})	a (AU)	δ_a^{obs} (AU)	δ_a^{theo} (AU)
HD 12661b	2.30 ± 0.19	0.831 ± 0.048	(1)	2.176	0.024	0.028	0.8079	0.0001	0.0052
HD 12661c	1.92 ± 0.16	2.90 ± 0.17	(1)	1.812	0.042	0.023	2.8145	0.0153	0.0182
HD 50554b	5.16	2.41	(2)	4.954	0.388	0.031	2.3530	0.0446	0.0075
HD 82943b	1.59	1.1866	(3)	1.500	0.067	0.009	1.1510	0.0053	0.0036
HD 82943c	1.58	0.7423	(3)	1.500	0.071	0.009	0.7209	0.0017	0.0023
HD 82943d	0.294 ± 0.031	2.137 ± 0.017	(4)	0.278	0.030	0.001	2.0766	0.0167	0.0066
HD 89307b	2.0 ± 0.4	3.34 ± 0.17	(5)	2.074	0.356	0.013	3.3632	0.0619	0.0106
HD 106252b	7.56	2.70	(2)	7.613	0.364	0.147	2.7033	0.0202	0.0259
HD 141937b	9.7	1.52	(6)	9.316	0.306	0.120	1.4877	0.0018	0.0095

Reference: (1) Wright et al. (2009); (2) Perrier et al. (2003); (3) Tan et al. (2013); (4) Baluev & Beaugé (2014); (5) Boisse et al. (2012); (6) Udry et al. (2002).

5 DISCUSSION AND CONCLUSION

We made an investigation of the physical state of the six EH stars and their own planet, by employing the method presented by do Nascimento et al. (2009). In the context of commonly observations we added two observational constraints, the lithium abundance $\log N(\text{Li})$ and the rotational period P_{rot} , as constraints to better determine the fundamental parameters of EH stars and their planets.

We gave the estimations of stellar masses and ages using only the effective temperature T_{eff} and luminosity L/L_{\odot} as observation constraints. The uncertainties of the mass and age are approximately $0.05 M_{\odot}$ and 4.0 Gyr. As we considered the lithium abundance $\log N(\text{Li})$ and rotational period P_{rot} in our analysis, we obtained more precise determinations. The lithium abundance helped us to minimize the errors of masses and ages to $0.03 M_{\odot}$ and 3.0 Gyr, respectively. Additionally, we used the rotational period P_{rot} to restrict stellar models based on the former results. The precision has been improved with $\Delta M \sim 0.02 M_{\odot}$ and $\Delta t \sim 0.5$ Gyr. Furthermore, because of the precise determination of age, we restricted atmospheric characteristics more strictly than the observations, and positioned the stars more exactly in the H-R diagram. Furthermore, we obtained the accurate planetary parameters, i.e., minimum masses $M_2 \sin i$ and orbital semimajor axes a by using RV measurements and stellar masses determined previously.

If we want to completely characterize a system, and obtain accurate properties of the planet, i.e., the mass, radius, and density, we need the photometric transit, the RV observations and the properties of EH star. In the future, we hope to conduct further studies with the data from Gaia mission.

Acknowledgements This work is supported by the grants 10933002, 11273007 and 11273012 from the National Natural Science Foundation of China, and the Fundamental Research Funds for the Central Universities.

References

- Angulo, C., Arnould, M., Rayet, M., et al. 1999, Nucl. Phys. A, 656, 3
Baluev, R. V., & Beaugé, C. 2014, MNRAS, 439, 673
Baranne, A., Queloz, D., Mayor, M., et al. 1996, A&AS, 119, 373
Batalha, N. M., Rowe, J. F., Bryson, S. T., et al. 2013, ApJS, 204, 24
Baumann, P., Ramírez, I., Meléndez, J., Asplund, M., & Lind, K. 2010, A&A, 519, A87
Bi, S. L., Basu, S., & Li, L. H. 2008, ApJ, 673, 1093
Böhm-Vitense, E. 1958, ZAp, 46, 108
Boisse, I., Pepe, F., Perrier, C., et al. 2012, A&A, 545, A55
Bouvier, J., Forestini, M., & Allain, S. 1997, A&A, 326, 1023

- Castro, M., do Nascimento, J. D., Jr., Biazzo, K., et al. 2011, *A&A*, 526, A17
- Chaboyer, B., Demarque, P., Guenther, D. B., et al. 1995, *ApJ*, 446, 435
- Demarque, P., Guenther, D. B., Li, L. H., Mazumdar, A., & Straka, C. W. 2008, *Ap&SS*, 316, 31
- Diego, F., Charalambous, A., Fish, A. C., & Walker, D. D. 1990, *Proc. SPIE*, 1235, 562
- do Nascimento, J. D., Jr., Castro, M., Meléndez, J., et al. 2009, *A&A*, 501, 687
- Eggenberger, P., Meynet, G., Maeder, A., et al. 2010, *A&A*, 519, A116
- Ferguson, J. W., Alexander, D. R., Allard, F., et al. 2005, *ApJ*, 623, 585
- Ghezzi, L., Cunha, K., Smith, V. V., et al. 2010a, *ApJ*, 720, 1290
- Ghezzi, L., Cunha, K., Smith, V. V., & de la Reza, R. 2010b, *ApJ*, 724, 154
- Grevesse, N., & Sauval, A. J. 1998, *Space Sci. Rev.*, 85, 161
- Guenther, D. B., Demarque, P., Kim, Y. C., Pinsonneault, M. H. 1992, *ApJ*, 387, 372
- Israelian, G., Santos, N. C., Mayor, M., & Rebolo, R. 2004, *A&A*, 414, 601
- Kaufer, A., Stahl, O., Tubbesing, S., et al. 1999, *The Messenger*, 95, 8
- Kawaler, S. D. 1988, *ApJ*, 333, 236
- Li, L. H., Basu, S., Sofia, S., et al. 2003, *ApJ*, 591, 1267
- Li, T. D., Bi, S. L., Chen, Y. Q., et al. 2012, *ApJ*, 746, 143
- Meléndez, J., Ramírez, I., Casagrande, L., et al. 2010, *Ap&SS*, 328, 193
- Moutou, C., Mayor, M., Lo Curto, G., et al. 2011, *A&A*, 527, A63
- Ofir, A., & Dreizler, S. 2013, *A&A*, 555, A58
- Perrier, C., Sivan, J.-P., Naef, D., et al. 2003, *A&A*, 410, 1039
- Pietrukowicz, P., Minniti, D., Díaz, R. F., et al. 2010, *A&A*, 509, A4
- Pinsonneault, M. H., Kawaler, S. D. & Demarque, P. 1990, *ApJS*, 74, 501
- Pinsonneault, M. H., Deliyannis, C. P. & Demarque, P. 1992, *ApJS*, 78, 179
- Queloz, D., Mayor, M., Weber, L., et al. 2000, *A&A*, 354, 99
- Rogers, F. J., & Nayfonov, A. 2002, *ApJ*, 576, 1064
- Rowe, J. F., Bryson, S. T., Marcy, G. W., et al. 2014, *ApJ*, 784, 45
- Santos, N. C. 2008, *New Astron. Rev.*, 52, 154
- Santos, N. C., Delgado Mena, E., Israelian, G., et al. 2010, in *IAU Symp. 268, Light Elements in the Universe*, ed. C. Charbonnel et al. (Cambridge: Cambridge Univ. Press), 291
- Seager, S., & Mallén-Ornelas, G. 2003, *ApJ*, 585, 1038
- Tan, X. Y., Payne, M. J., Lee, M. H., et al. 2013, *ApJ*, 777, 101
- Thoul, A. A., Bahcall, J. N., & Loeb, A. 1994, *ApJ*, 421, 828
- Udry, S., Mayor, M., Naef, D., et al. 2000, *A&A*, 356, 590
- Udry, S., Mayor, M., Naef, D., et al. 2002, *A&A*, 390, 267
- Valenti, J. A. & Fischer, D. A. 2005, *ApJS*, 159, 141
- Vogt, S. S. 1987, *PASP*, 99, 1214
- Vogt, S. S., Allen, S. L., Bigelow, B. C., et al. 1994, *Proc. SPIE*, 2198, 362
- Vogt, S. S., Marcy, G. W., Butler, R. P., & Apps, K. 2000, *ApJ*, 536, 902
- Winn, J. N. 2010, in *Exoplanets*, ed. S. Seager (Tucson, AZ: Univ. Arizona Press) arXiv:1001.2010
- Wright, J. T., Marcy, G. W., Butler, R. Paul, & Vogt, S. S. 2004, *ApJS*, 152, 261
- Wright, J. T., Upadhyay, S., Marcy, G. W., et al. 2009, *ApJ*, 693, 1084